Supplementary information: In-situ error analysis in contact angle goniometry

Heikki A. Nurmi, Gentrit Zenuni, Sakari Lepikko, Reetta Saine, Maja Vuckovac, and Robin H. A. Ras

Preparation of samples

Fluorinated silver-coated copper

The fluorinated silver-coated copper surface was prepared as described by Timonen et al[1] using the chemicals (99% $AgNO_3$, Fluka, 97% 1*H*,1*H*,2*H*,2*H*-perfluorodecanethiol, Aldrich, and 99% 1,2-dichloromethane, Aldrich) as obtained. A silver coating was applied on a mechanically polished copper substrate by immersing it into an aqueous 0.01 M $AgNO_3$ solution for 60 s. The surface was washed with Milli-Q water and dried under N_2 flow, followed by immersing it into a 0.001 M solution of 1*H*,1*H*,2*H*,2*H*-perfluorodecanethiol in 1,2-dichloromethane for 10 min. Last, the surface was washed twice with fresh 1,2-dichloromethane and let dry under ambient conditions.

Silicon micropillars on Si wafer coated with fluoropolymer

The surface was prepared as described by Liimatainen et al. [2] using deep reactive ion etching to fabricate the silicon micropillars. A plasma-enhanced chemical vapor deposited (PECVD) oxide (Oxford PlasmaLab 80+, 300°C, 8.5 sccm SiH_4, 1000 mTorr, 20 W) was deposited on silicon wafer (4-inch, <100>, p-type doping 1-20 ohm-cm) with a 12-minute deposition time and oxide thickness of 750 nm. A pillar pattern with a pillar radius of 5 µm was formed by UV lithography and reactive ion etching (Oxford PlasmaLab 80+, 25 sccm Ar, 25 sccm CHF_3, 200 W, 30 mTorr, 21 min etching time). Cryogenic deep reactive ion etching (Oxford PlasmaLab System 100, -110 °C, 40 sccm SF_6, 6 sccm O2, 1050 W ICP power, 3 W platen power, 8 mTorr) was used to etch the silicon pillars with an etch depth of 20 µm, followed by removing the oxide mask with hydrofluoric acid and depositing a thin layer of hydrophobic fluoropolymer on top of the pillars by PECVD (Oxford PlasmaLab 80+, 100 sccm CHF_3, 50 W, 30 mTorr) with a 5-minute deposition time. The micropillars used here had a center-to-center spacing of 120 µm.

Silicone nanofilaments on Si wafer

The surface was prepared as described by Liimatainen et al. [2]. Silicone nanofilaments were fabricated by chemical vapor deposition on silicon <100> wafer. The wafer was ultrasonicated in an alkaline solvent (Deconex 11 Universal, VWR). Then, the wafer was washed with Milli-Q water and the surface was dried under N_2 flow. Chemical vapor deposition was performed in an in-house built gas-phase reactor at atmospheric pressure. The reactor was first purged with dry argon, followed by pre-humidified argon.

The reactor was sealed when the relative humidity reached ca. 30%, after which methyltrichlorosilane (2 µl, 99%, Aldrich) was injected and let to evaporate to grow the nanofilaments onto the surface.

Contact angle measurement procedure

The contact angle measurements were conducted according to the protocol[3] using a commercial goniometer (Biolin Scientific, model Attension Theta). The sample surfaces were cleaned by blowing under pressurized N_2 flow to remove any dust, and ultrapure Milli-Q water was dispensed into a clean glass container. The samples and the probe liquid were kept in the ambient conditions of the laboratory (approximately 20°C and 1 atm) during the setup preparation (15-30 minutes) to allow them to attain a uniform temperature. The camera and sample stage of the goniometer were verified to be completely horizontal with a spirit level. The imaging system was calibrated using the goniometer's calibration sphere.

One measurement cycle includes both an advancing and a receding contact angle (ACA, RCA) measurement. Three repeat measurement cycles on varying locations were conducted on each sample to diminish the effect of spatial heterogeneity. When a droplet volume range is reported here, it stands for a value picked within the range, which is suitable for the specific sample in the measurements.

In an ACA measurement, a 1 µl droplet was dispensed to hang from the tip of the needle. The needle was lowered and adjusted to display the droplet in the middle of the camera view. The sample stage was raised to bring the droplet into contact with the sample until the tip of the needle was in the middle of the droplet. At a flow rate of 0.05 µl/s, 1 µl was dispensed into the droplet, resulting in a size of 2 µl. The flow rate remained constant at this value for the entire procedure. Recording the ACA video was started, followed by dispensing 10-15 µl. The recording was stopped after the dispensing had finished.

An RCA measurement was started by adding 2-5 µl (with a flow rate of 1µl/s) into the droplet grown during the ACA measurement to reach a suitable starting volume. If needed, the positions of the sample stage and the needle were readjusted into a configuration equivalent to the ACA measurement. Recording of the RCA video was started, followed by withdrawing 15-18 µl (with a flow rate of 0.05 µl/s) from the droplet. After the withdrawal had finished, the recording was stopped. The sample stage was lowered, and any remaining water was cleaned off the sample. 30 µl was dispensed to a wipe to replace the water already used for measurements before proceeding to the next measurement.

Rotational misalignment between sample stage and camera

The rotational misalignment between the sample stage and camera (Figure S1) needs to be considered when analyzing the contact angle of a droplet. This misalignment is calculated from the slope of the baseline and included into the contact angle as described in the manuscript. This rotational misalignment originates mainly from the tilt of sample stage and the possible varying thickness of the sample itself and minor part of it comes from the misalignment of the camera in its holder. One way to minimize the misalignment is to level the sample stage before each measurement, however in general this needs to be considered in contact angle analysis.

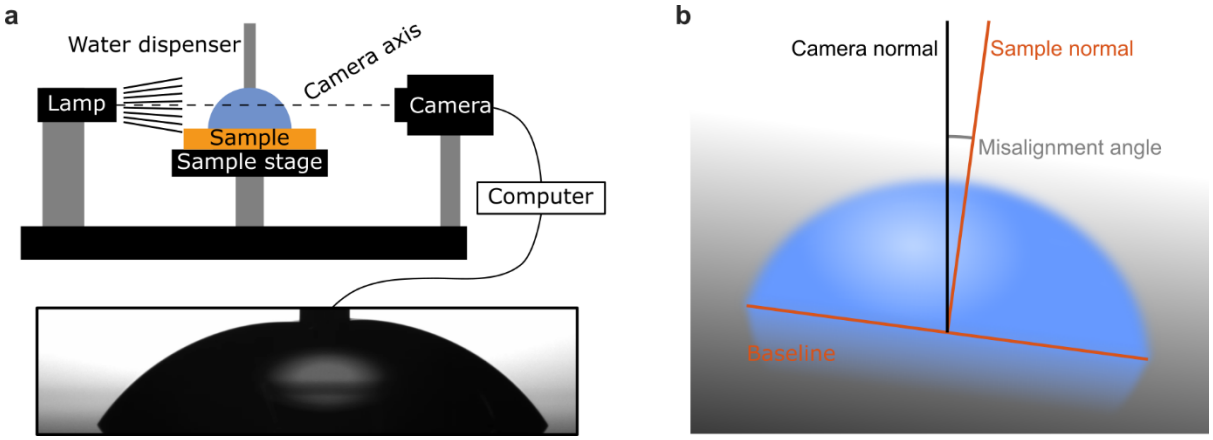

Figure S1. Schematic of the misalignment along the camera axis between the camera and the sample in contact angle goniometer. ***a*** *Schematic of contact angle goniometer and an example photo of a droplet.* ***b*** *Misalignment angle between the camera normal and sample normal. The sample normal is assumed to be against the baseline.*

Baseline detection of 80° to 120° contact angle droplets

The issue of baseline detection between 80° and 120° has to do with the near circular shape of the droplet shadow and the background gradient. This causes the Harris measure to have only slightly positive values, or the positive values elongate along with the droplet edge upwards or downwards. This then causes the corner to be detected at an incorrect location. Figures S2 and S3 show an example of this, where a real droplet with contact angle around 110° and a simulated droplet of 95°, along with the Harris measure near the contact point. The Harris measure values below zero are set as zero for visualization purposes.

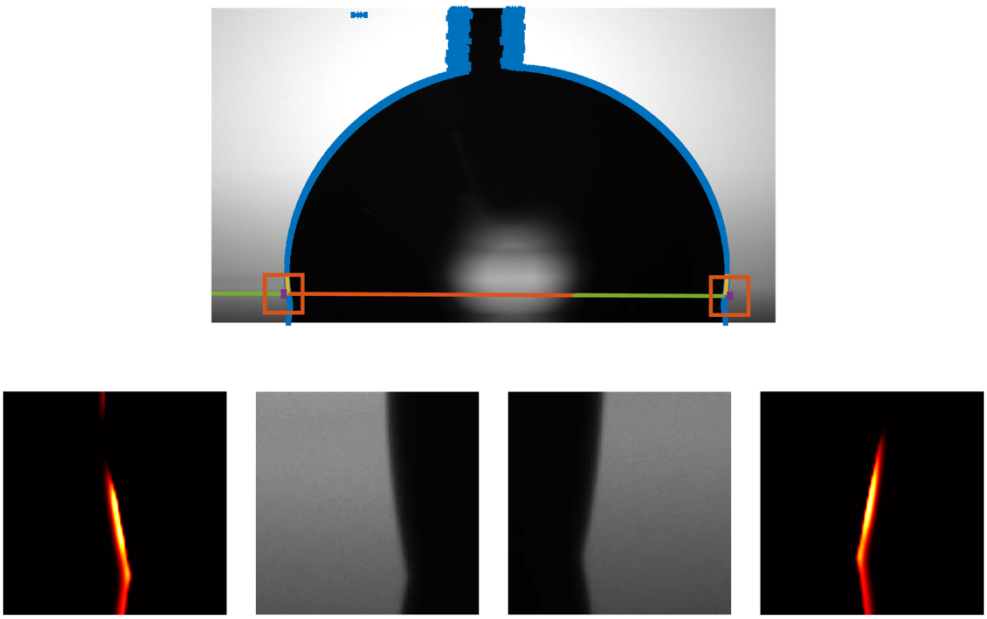

Figure S2. Frame of contact angle measurement from octyltrichlorosilane self-assembled monolayer sample and the analyzed Harris measure. Small values black and higher values from red to yellow to white. High values correspond to a corner.

In Figure S2, the contact angle analysis fails, as the polynomial fit (yellow) of the edge (blue points with error bars) starts to rise before the baseline (red line). This causes the analysis to give contact angles of roughly 180° (left) and 0° (right) depicted with green lines. This failure to analyze is due to the bad contact point detection and failure to find the intersection of the polynomial fit and the baseline. The red rectangles show the location of the insets on the bottom row, which have the Harris measure and the plain image of the droplet. The large values of the Harris measure (and the maximum value is in the center of the insets) are higher than the visually correct contact point, which is visible as a smaller area, more circular of positive values.

Figure S3 shows a simulated droplet with insets showing Harris measure and the raw image of the contact point areas. In this case, the Harris measure is spread out much more evenly compared to Figure S2 and highlights the issue of corner detection even better when the droplet and its shadow form a near circular combination i.e., contact angles around 80° to 100°. The contact angle analysis gives reasonable values in this case, as can be seen from the green lines depicting the contact angle; however, due to the invalid detection of contact point, these values are meaningless. In the Harris measure, there is a large spread in the y-direction of the large values, which both increase the uncertainty of the actual maximum point and causes the maximum to be sensitive to any small variations in the corner measure. The contact point is difficult to pinpoint in all insets where are the Harris measure and the raw image of the simulated droplet from both sides.

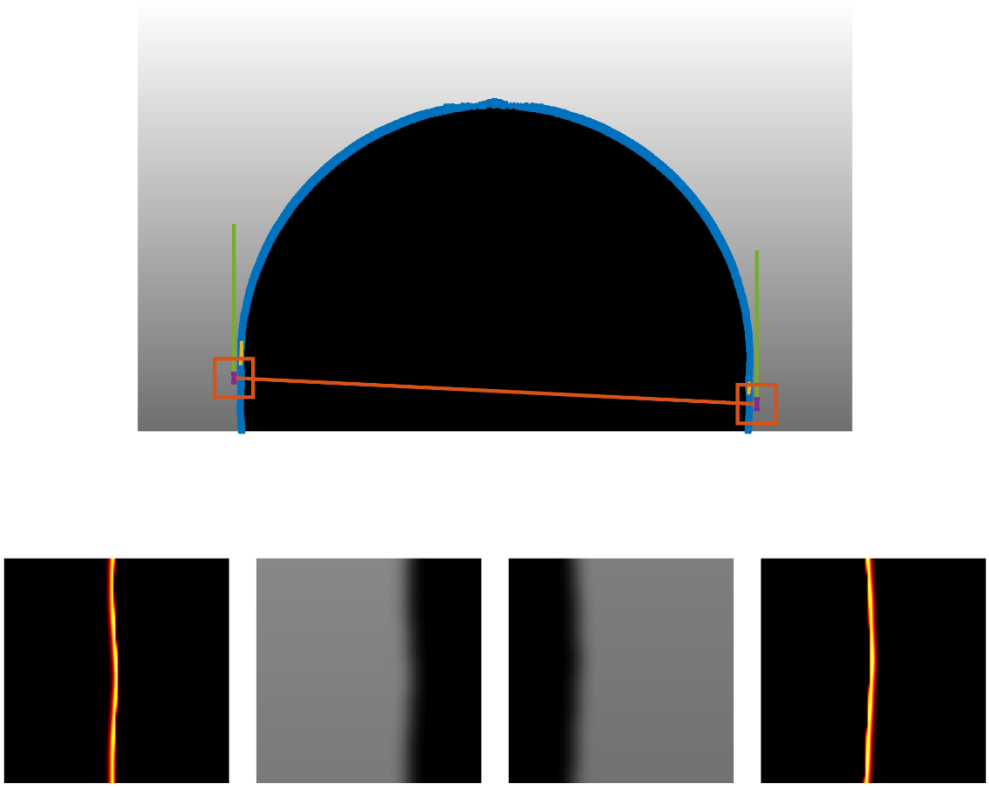

Figure S3. Simulated droplet contact angle and the analyzed Harris measure. Small values black and higher values from red to yellow to white. High values correspond to a corner.

Analysis of simulated droplets with varying misalignment angles

We explored the effect of tilted surface with the simulated droplets by rotating the image of the simulated droplet by angles between -5° and 5° before analyzing it. The rotated simulated droplets were created based on the binary images by first rotating the image by a set angle and then filling the background image to be rectangle again. The implementation can be found in the script `analyseSyntheticDrops.m`. Then the blur and background were added to the image as described in the main text.

The analysis results of the rotated droplets can be found in Figure S4, which shows the in-situ errors of correct contact angle and misalignment angle for the simulated droplets. The code has issues finding the correct contact angle around 80° and 100° due to the droplet being nearly circular, however the analysis also correctly identifies this by having large in-situ errors with this range. There is a systematic overestimation of analyzed the contact angles of the simulated droplets below 90° and systematic under estimation for angles above 90°. However, this magnitude is typically low (below 2°) and there is no clear correlation between the in-situ error of contact angle and the given misalignment angle. The misalignment is detected accurately with all misalignment angles, however, there is

large uncertainty when the contact angle is near 90° and no clear corner can be detected near the contact point.

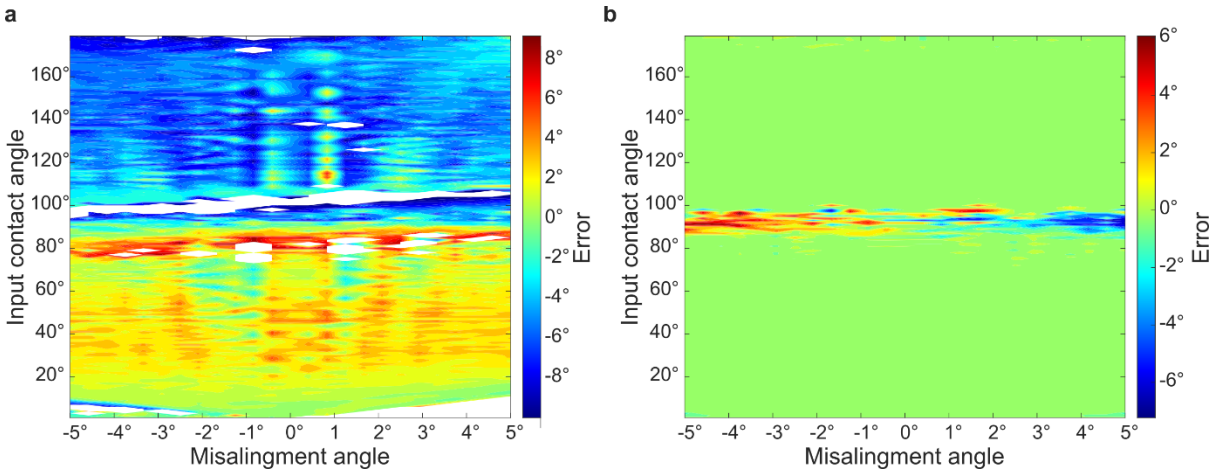

Figure S4. Errors of the measured contact angle and misalignment of droplet of the analyzed simulated droplets. ***a*** *Error of measured contact angle for simulated droplets with given contact angle and misalignment angle. White areas stand for areas having errors larger than 10° in magnitude.* ***b*** *Error of measured misalignment angle for simulated droplets with given contact and misalignment angle.*

Contact point detection failure examples

The contact point detection was considered failed if the distance between the polynomial and the baseline at smallest was larger than 20 pixels. Example of this is shown in Figure S5, where cases of differences of 35, 250, 60 000 and 100 000 px is showed. These fitting failures could be due to various reasons: dust particles and reflection of the light source in the image Figure S5c, needle in the image Figure S5b. These can be considered as bugs in the code and could be resolved using more advanced corner detection logic than finding the strongest corner in each half. However, the failure in Figure S5d is due to extremely low contact angle. It should be noticed that these issues are mostly with droplets having contact angle around 90°, where the corner strength is weak.

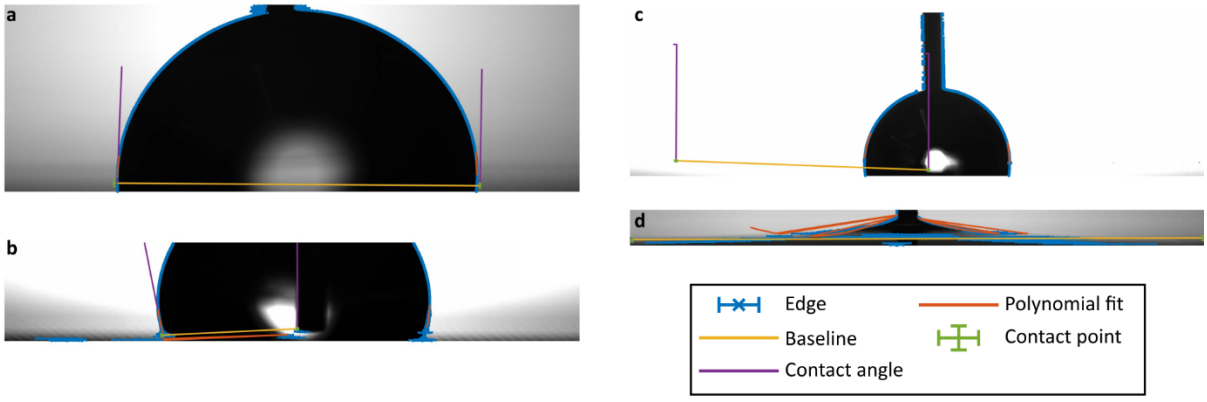

*Figure S5. Contact point detection failure examples. The following droplets had issues detecting the real contact points and had larger than 20 px difference between the polynomial fit and the baseline (****a*** *35 px,* ***b*** *100 000,* ***c*** *60 000 and* ***d*** *250). Only the 35 px example show a contact angle that can be considered passable, while the larger differences show clear failures for fitting.*

References

1. Timonen, J. V. I., Latikka, M., Ikkala, O. & Ras, R. H. A. Free-decay and resonant methods for investigating the fundamental limit of superhydrophobicity. *Nat Commun* **4**, 2398 (2013).

2. Liimatainen, V. *et al*. Mapping microscale wetting variations on biological and synthetic water-repellent surfaces. *Nat Commun* **8**, 1798 (2017).

3. Huhtamäki, T., Tian, X., Korhonen, J. T. & Ras, R. H. A. Surface-wetting characterization using contact-angle measurements. *Nat Protoc* **13**, 1521–1538 (2018).